Smart-Tree: Neural Medial Axis Approximation of Point Clouds for 3D Tree Skeletonization ⋆

Harry Dobbs[1][0000−0003−3685−940X], Oliver Batchelor[2][0000−0002−6542−1661], Richard Green[2][0000−0001−5149−722X], and James Atlas[2][0000−0002−8030−6098]

UC Vision Research Lab,
University of Canterbury,
Christchurch 8041, New Zealand
`harry.dobbs@pg.canterbury.ac.nz`
{`oliver.batchelor, richard.green, james.atlas`}`@canterbury.ac.nz`
`https://ucvision.org.nz/`

Abstract. This paper introduces Smart-Tree, a supervised method for approximating the medial axes of branch skeletons from a tree point cloud. Smart-Tree uses a sparse voxel convolutional neural network to extract the radius and direction towards the medial axis of each input point. A greedy algorithm performs robust skeletonization using the estimated medial axis. Our proposed method provides robustness to complex tree structures and improves fidelity when dealing with self-occlusions, complex geometry, touching branches, and varying point densities. We evaluate Smart-Tree using a multi-species synthetic tree dataset and perform qualitative analysis on a real-world tree point cloud. Our experimentation with synthetic and real-world datasets demonstrates the robustness of our approach over the current state-of-the-art method. The dataset[1] and source code[2] are publicly available.

Keywords: Tree Skeletonization · Point Cloud · Metric Extraction · Neural Network.

1 Introduction

Digital tree models have many applications, such as biomass estimation [14,22,13], growth modelling [33,31,7], forestry management [35,25,3], urban microclimate simulation [36], and agri-tech applications, such as robotic pruning [38,2], and fruit picking [1].

A comprehensive digital tree model relies on the ability to extract a skeleton from a point cloud. In general, a skeleton is a thin structure that encodes an object's topology and basic geometry [6]. Skeleton extraction from 3D point clouds has been studied extensively in computer vision and graphics literature [30] for understanding shapes and topology. Applied to tree point clouds, this is a

---

⋆ Supported by University of Canterbury, New Zealand.

[1] `https://github.com/uc-vision/synthetic-trees`

[2] `https://github.com/uc-vision/smart-tree`

challenging problem due to self-occlusions, complex geometry, touching branches, and varying point densities.

There are many existing approaches for recovering tree skeletons from point clouds (recent survey [5]). These approaches can be categorized as follows; neighbourhood graph, medial axis approximation, voxel and mathematical morphology, and segmentation.

Neighbourhood graph methods use K-nearest neighbours (usually within a search radius) or Delaunay triangulation to create an initial graph from the point cloud. Multiple implementations [34,37,11,19], then use this graph to quantize the points into bins based on the distance from the root node. The bin centroids are connected based on constraints to create a skeleton. Livny et al. [24] use the neighbourhood graph to perform global optimizations based on a smoothed orientation field. Du et al. [12] use the graph to construct a Minimum Spanning Tree (MST) and perform iterative graph simplification to extract a skeleton. However, these methods have some drawbacks. Gaps in the point cloud, such as those caused by occlusions, can lead to a disconnected neighbourhood graph. Additionally, false connections may occur, especially when branches are close to one another.

Medial axis approximation works by estimating the medial surface and then thinning it to a medial axis. An approach in the *L1-Medial Skeleton* method [20] was proposed for point clouds by iterative sampling and redistributing points to the sample centre. Similarly, Cao et al. [4] proposed using Laplacian-based contraction to estimate the medial axis. However, these methods are sensitive to irregularities in the point cloud and require a densely sampled object as input.

Voxel and mathematical morphology were implemented in [16] and later refined in [15]. The point cloud is converted into a 3D voxel grid and then undergoes opening and closing, resulting in a thinned voxel model. The voxel spatial resolution is a key parameter, as a too-fine resolution will lead to many holes. In contrast, a larger resolution can lose significant detail as multiple points become a single voxel (different branches may all become connected). A further limitation of this method is the required memory and time, which increases with the third power of the resolution. This method only aims to find prominent structures of trees rather than finer branches.

Segmentation approaches work by segmenting points into groups from the same branch. Raumonen [28] et al. create surface patches along the tree and then grow these patches into branches. However, this method assumes that local areas of the tree have a uniform density.

Recently a deep learning segmentation approach was proposed in TreePartNet [23]. This method uses two networks, one to detect branching points and another to detect cylindrical representations. It requires a sufficiently sampled point cloud as it relies on the ability to detect junctions accurately and embed local point groups. However, it struggles to work on larger point clouds due to the memory constraints of PointNet++ [27]. Numerous network architectures can process point clouds [18]; however, point clouds in general, but in particu-

lar, trees are spatially large and sparse, containing fine details - for this reason, we utilise submanifold sparse CNNs [17,9,32,8].

We propose a deep-learning-based method to estimate the medial axis of a tree point cloud. A neighbourhood graph approach is then used to extract the skeleton. This method mitigates the effects of errors commonly caused when neighbouring branches get close or overlap, as well as improving robustness to common challenges such as varying point density, noise and missing data. Our contributions are as follows:

– A synthetic point cloud generation tool was developed for creating a wide range of labelled tree point clouds.
– A demonstration of how a sparse convolutional neural network can effectively predict the position of the medial axis.
– A skeletonization algorithm is implemented that can use the information from the neural network to perform a robust skeletonization.
– The method is evaluated against the state-of-the-art automatic skeletonization method.
– The method's ability to generalize is demonstrated by applying it to real data.

2 Method

2.1 Dataset

We use synthetic data for multiple reasons. First, it has a known ground truth skeleton for quantitative evaluation. Second, we can efficiently label the point clouds - allowing us to generate data for a broad range of species.

We create synthetic trees using a tree modelling software called SpeedTree [21]. For evaluation, we generate the tree meshes without foliage, which otherwise increase the level of occlusion. In the general case, we remove foliage using a segmentation step. Generating point clouds from the tree meshes is done by emulating a spiral drone flight path around each tree and capturing RGBD images at a resolution of 2.1 megapixels (1920 x 1080 pixels).

We randomly select a sky-box for each tree for varying lighting conditions. The depth maps undergo augmentations such as jitter, dilation and erosion to replicate photogrammetry noise. We extract a point cloud from the fused RGBD images. We remove duplicate points by performing a voxel downsample at a 1cm resolution. The final point clouds have artefacts such as varying point density, missing areas (some due to self-occlusion) and noise.

We select six species with SpeedTree models. We produce 100 point clouds (600 total) for each of the six tree species, which vary in intricacy and size. Of these, 480 are used for training, while 60 are reserved for validation and 60 for testing. We show images of the synthetic point cloud dataset in the results section (Section 3). Future revisions will include point clouds with foliage and a wider variety of species.

2.2   Skeletonization Overview

Our skeletonization method comprises several stages shown in Figure 2. We use labelled point clouds to train a sparse convolutional neural network to predict each input point's radius and direction toward the medial axis (ground truth skeleton). Using these predictions, we then translate surface points to estimated medial axis positions and construct a constrained neighbourhood graph. We extract the skeleton using a greedy algorithm to find paths from the root to terminal points. The neural network predictions help to avoid ambiguities with unknown branch radii and separate points which would be close in proximity but from different branches.

2.3   Neural Network

Our network takes an input set of N arbitrary points $\{Pi|i = 1, ..., N\}$, where each point Pi is a vector of its (x, y, z) coordinates plus additional features such as colour (r, g, b). Each point is voxelized at a resolution of 1cm. Our proposed network will then, for each voxelized point, learn an associated radius $\{Ri|i = 1, ..., N\}$ where Ri is a vector of corresponding radii and a direction vector $\{Di|i = 1, ..., N\}$ where Di is a normalized direction vector pointing towards the medial axis.

The network is implemented as a submanifold sparse CNN using SpConv [9], and PyTorch [26]. We use regular sparse convolutions on the encoder blocks for a wider exchange of features and submanifold convolutions elsewhere for more efficient computation due to avoiding feature dilation. The encoder block uses a stride of 2. Each block uses a kernel size of 3x3x3, except for the first submanifold convolution and the fully connected blocks, which use a kernel size of 1x1x1.

The architecture comprises a UNet backbone [29] with residual connections, followed by two smaller fully connected networks to extract the radii and directions. A ReLU activation function and batch normalization follow each convolutional layer. We add a fully-connected network head when branch-foliage segmentation is required.

A high-level overview of the network architecture is shown in Figure 1.
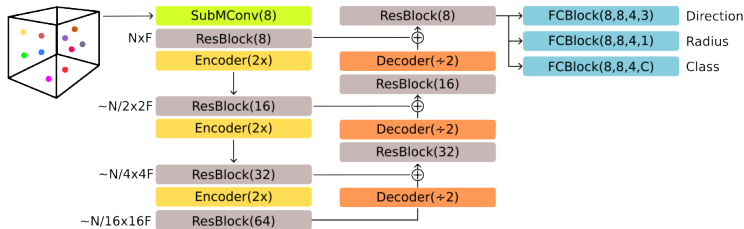
Fig. 1: Network architecture diagram.

A block sampling scheme ensures the network can process larger trees. During training, for each point cloud, we randomly sample (at each epoch) a $4m^3$ block and mask the outer regions of the block to avoid inaccurate predictions from the edges. We tile the blocks during inference, overlapping the masked regions.

We estimate a logarithmic radius to handle the variation in branch radii, which spans several orders of magnitude [10], which provides a relative error. The loss function (Equation 3) comprises two components. Firstly we use the L1-loss for the radius (Equation 2) and the cosine similarity (Equation 1) for the direction loss. We use the Adam optimizer, a batch size of 16, and a learning rate of 0.1. The learning rate decays by a factor of 10 if the validation data-set loss does not improve for 10 consecutive epochs.

$$L_D = \sum_{i=0}^{n} \frac{Di \cdot \hat{D}i}{||Di||_2 \cdot ||\hat{D}i||_2} \quad (1) \qquad L_R = \sum_{i=0}^{n} |\ln(Ri) - \hat{R}i| \quad (2)$$

$$Loss = L_R + L_D \tag{3}$$

2.4   Skeletonization Algorithm
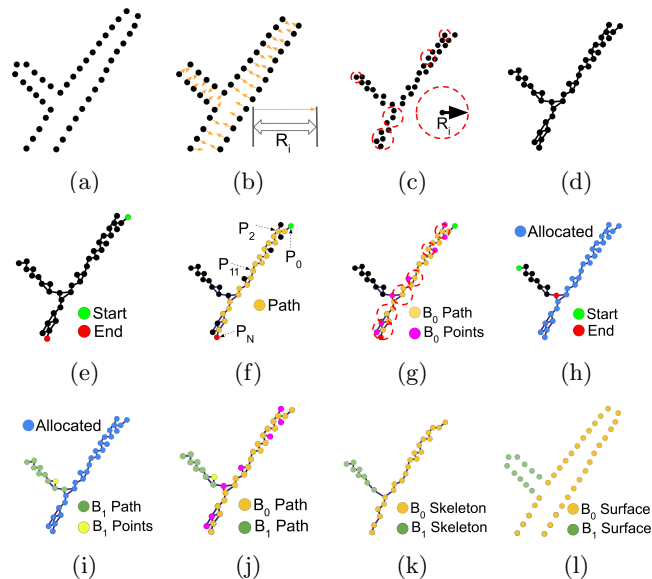
Fig. 2: Skeletonization Algorithm: (a) Input points, (b) Medial axis approximation, (c) Neighbourhood radius search, (d) Neighbourhood graph, (e) B_0 Farthest point, (f) B_0 Trace path,(g) B_0 Allocated points, (h) B_1 Farthest (unallocated) point, (i) B_1 Trace path and allocated points, (k) Branch skeletons, (i) Corresponding surface points.

Once $\{Ri\}$ and $\{Di\}$, have been predicted by the network. We use this information to project the input surface points $\{Pi\}$ (2a) onto the medial axis (2b).

We form a neighbourhood graph (2d) where points are connected to neighbours with weight equal to the distance between points and restricted to edges with a distance less than the predicted radius (2c).

As the point cloud has gaps due to self-occlusion and noise, we end up with multiple connected components. Each connected component we call a sub-graph. We process each sub-graph sequentially. For each sub-graph:

1. A distance tree is created based on the distance from the root node (the lowest point in each sub-graph - shown in red in (2e)) to each point in the sub-graph.
2. We assign each point a distance based on a Single Source Shortest Path (SSSP) algorithm. A greedy algorithm extracts paths individually until all points are marked as allocated (steps e to j).
3. We select a path to the furthest unallocated point and trace its path back to either the root (2e) or an allocated point (2i).
4. We add this path to a skeleton tree (2f).
5. We mark points as allocated which lie within the predicted radius of the path (2g).
6. We repeat this process until all points are allocated (2i, 2j)

3   Results

Performance evaluation of skeletonization algorithms is incredibly challenging and remains an open problem. Hence, there is no widely accepted metric used for evaluation. We compare our algorithms skeleton for quantitative evaluation using a form of precision and recall which matches points along the ground truth skeleton against points along the estimated skeleton.

We evaluate our method against the state-of-the-art AdTree algorithm [12]. As our metrics do not evaluate topological errors directly, additional qualitative analysis is conducted by visually inspecting the algorithm outputs against the ground truth.

Due to augmentations, some of the finer branches may become excessively noisy or disappear. To ensure the metrics measure what is possible to reconstruct, we prune the ground truth skeleton and point cloud based on a branch radius and length threshold - respective to tree size.

3.1   Metrics

We evaluate our skeletons using point cloud metrics by sampling our skeletons at a 1mm resolution. We use the following metrics to assess our approach: f-score, precision, recall and AUC. For the following metrics, we consider $p \in \mathcal{S}$ points along the ground truth skeleton and $p^* \in \mathcal{S}^*$ points obtained by sampling the output skeleton. p_r is the radius at each point. We use a threshold variable t,

which sets the distance points must be within based on a factor of the ground truth radius. We test this over the range of $0.0 - 1.0$. The f-score is the harmonic mean of the precision and recall.

Skeletonization Precision To calculate the precision, we first get the nearest points from the output skeleton $p_i \in \mathcal{S}$ to the ground truth skeleton $p_j^* \in \mathcal{S}^*$, using a distance metric of the euclidean distance relative to the ground truth radius r_j^*. The operator $[\![.]\!]$ is the Iverson bracket, which evaluates to 1 when the condition is true; otherwise, 0.

$$d_{ij} = ||p_i - p_j^*|| \tag{4}$$

$$P(t) = \frac{100}{|S|} \sum_{i \in \mathcal{S}} [\![d_{ij} < t\, r_j^* \wedge \underset{k \in \mathcal{S}}{\forall}\, d_{ij} \leq d_{kj}]\!] \tag{5}$$

Skeletonization Recall To calculate the recall, we first get the nearest points from the ground truth skeleton $p_j^* \in \mathcal{S}^*$ to the output skeleton $p_i \in \mathcal{S}$. We then calculate which points fall inside the thresholded ground truth radius. This gives us a measurement of the completeness of the output skeleton.

$$R(t) = \frac{100}{|S^*|} \sum_{j \in \mathcal{S}^*} [\![d_{ij} < t\, r_j^* \wedge \underset{k \in \mathcal{S}^*}{\forall}\, d_{ij} \leq d_{ik}]\!] \tag{6}$$

3.2 Quantitative Results

We evaluate our method on our test set of sixty synthetic ground truth skeletons (made up of six species). Our results are summarized in Table 1 and illustrated in Figure 3. We compute the AUC for F1, precision, and recall using the radius threshold t ranging from 0 to 1.

Table 1: Skeletonization Results.

Metric	Smart-Tree	AdTree
Precision AUC	0.53	0.21
Recall AUC	0.40	0.38
F1 AUC	0.45	0.26

Smart-Tree achieves a high precision score, with most points being close to the ground truth skeleton (Fig. 3a). Compared to AdTree, Smart-Tree has lower recall at the most permissive thresholds, and this is due to Smart-Tree's inability to approximate missing regions of the point cloud, making it prone to

gaps. AdTree, on the other hand, benefits from approximating missing regions. However, this also leads to AdTree having more topological errors and lower precision. Smart-Tree consistently achieves a higher F1 score and AUC for precision, recall, and F1, respectively.
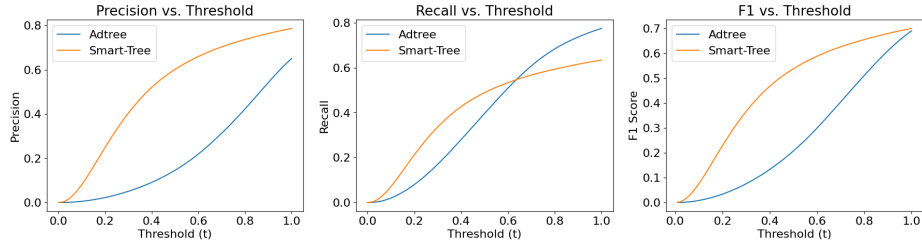
Fig. 3: Left to right: Precision Results (a), Recall Results (b), F1 Results (c).

3.3   Qualitative Results

In Figure 5, we show qualitative results for each species in our synthetic dataset. We can see that Smart-Tree produces an accurate skeleton representing the tree topology well. Adtree produces additional branches that would require post-processing to remove.

AdTree often fails to capture the correct topology of the tree. This is due to Adtree using Delaunay triangulation to initialise the neighbourhood graph. This can lead to branches that have no association being connected.

Smart-Tree, however, does not generate a fully connected skeleton - but rather one with multiple sub-graphs. The biggest sub-graph can still capture the majority of the major branching structure, although to provide a full topology of the tree with the finer branches, additional work is required to connect the sub-graphs by inferring the branching structure in occluded regions.

To demonstrate our method's ability to work on real-world data. We test our method on a tree from the Christchurch Botanic Gardens, New Zealand. As this tree has foliage, we train our network to segment away the foliage points and then run the skeletonization algorithm on the remaining points. In Figure 4c, we can see that Smart-Tree can accurately reconstruct the skeleton.

Fig. 4: Left to Right: Input point cloud (a), Branch meshes (b), Skeleton Subgraphs (c).
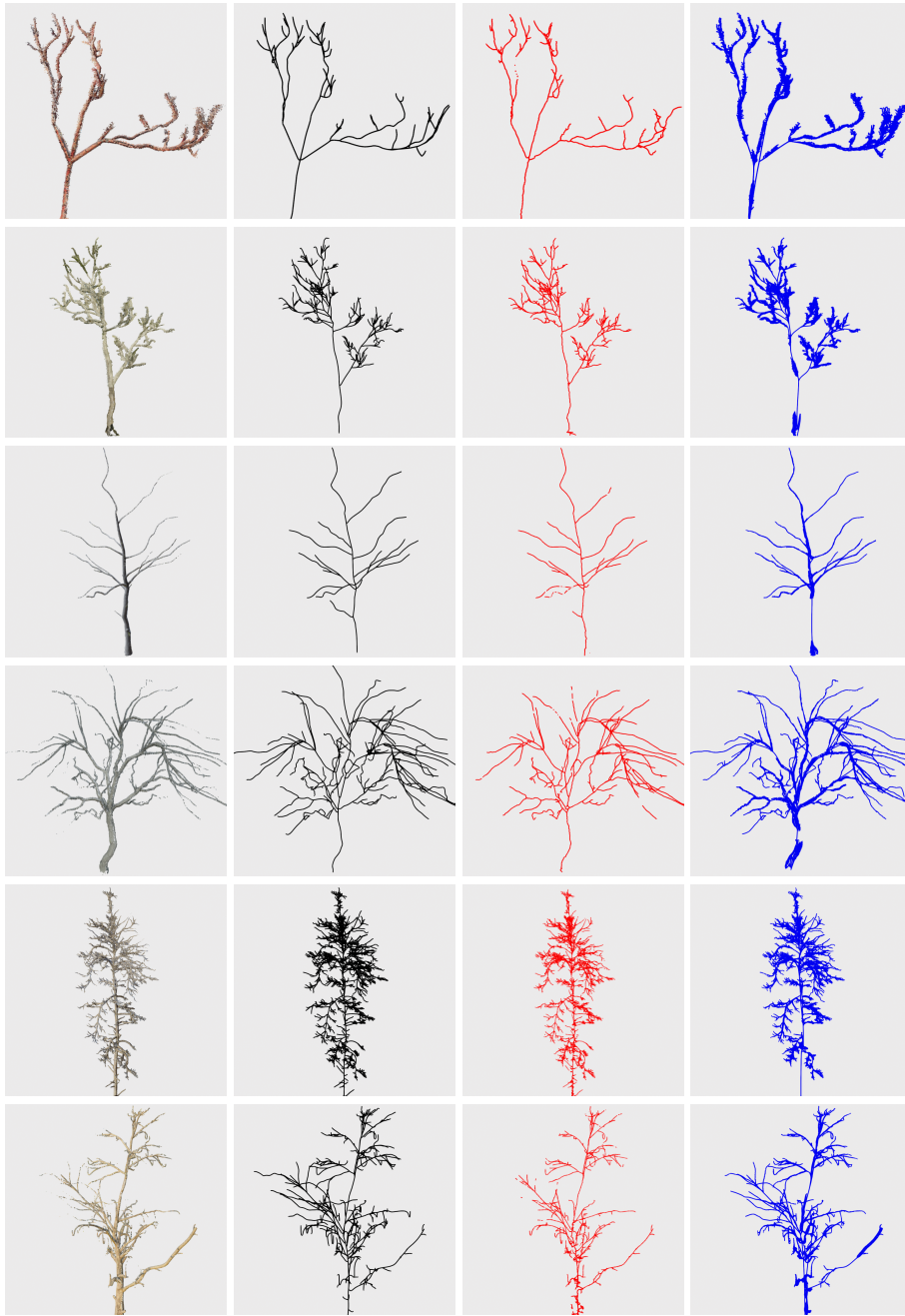
Fig. 5: Several results of skeletonization of synthetic point clouds. From left to right: synthetic point cloud, ground truth skeleton, Smart-Tree skeleton, and Adtree skeleton. From top to bottom (species): cherry, eucalyptus, walnut, apple, pine, ginkgo

4   Conclusion and Future Work

We proposed Smart-Tree, a supervised method for generating skeletons from tree point clouds. A major area for improvement in the literature on tree point-cloud skeletonization is quantitative evaluation, which we contribute towards with a synthetic tree point cloud dataset with ground-truth and error metrics.

We demonstrated that using a sparse convolutional neural network can help improve the robustness of tree point cloud skeletonization. One novelty of our work is that a neighbourhood graph can be created based on the radius at each region, improving the accuracy of our skeleton.

We used a precision and recall-based metric to compare Smart-Tree with the state-of-the-art AdTree. Smart-Tree is generally much more precise than AdTree, but it currently does not handle point clouds containing gaps (due to occlusions and reconstruction errors). AdTree has problems with over-completeness on this dataset, with many duplicate branches.

In the future, we would like to work towards robustness to gaps in the point cloud by filling gaps in the medial-axis estimation phase. We plan to train our method on a wider range of synthetic and real trees; to do this, we will expand our dataset to include more variety, trees with foliage, and human annotation on real trees. We are also working towards error metrics which better capture topology errors.

Acknowledgment

References

1. Arikapudi, R., Vougioukas, S.G.: Robotic tree-fruit harvesting with telescoping arms: a study of linear fruit reachability under geometric constraints. IEEE Access **9**, 17114–17126 (2021)
2. Botterill, T., Paulin, S., Green, R., Williams, S., Lin, J., Saxton, V., Mills, S., Chen, X., Corbett-Davies, S.: A robot system for pruning grape vines. Journal of Field Robotics **34**(6), 1100–1122 (2017)
3. Calders, K., Adams, J., Armston, J., Bartholomeus, H., Bauwens, S., Bentley, L.P., Chave, J., Danson, F.M., Demol, M., Disney, M., et al.: Terrestrial laser scanning in forest ecology: Expanding the horizon. Remote Sensing of Environment **251**, 112102 (2020)

4. Cao, J., Tagliasacchi, A., Olson, M., Zhang, H., Su, Z.: Point cloud skeletons via laplacian based contraction. In: 2010 Shape Modeling International Conference. pp. 187–197. IEEE (2010)

5. Cárdenas-Donoso, J.L., Ogayar, C.J., Feito, F.R., Jurado, J.M.: Modeling of the 3d tree skeleton using real-world data: A survey. IEEE Transactions on Visualization and Computer Graphics (2022)

6. Chaudhury, A., Godin, C.: Skeletonization of plant point cloud data using stochastic optimization framework. Frontiers in Plant Science **11**, 773 (2020)

7. Chaudhury, A., Ward, C., Talasaz, A., Ivanov, A.G., Brophy, M., Grodzinski, B., Hüner, N.P., Patel, R.V., Barron, J.L.: Machine vision system for 3d plant phenotyping. IEEE/ACM transactions on computational biology and bioinformatics **16**(6), 2009–2022 (2018)

8. Choy, C., Gwak, J., Savarese, S.: 4d spatio-temporal convnets: Minkowski convolutional neural networks. In: Proceedings of the IEEE/CVF Conference on Computer Vision and Pattern Recognition. pp. 3075–3084 (2019)

9. Contributors, S.: Spconv: Spatially sparse convolution library. `https://github.com/traveller59/spconv` (2022)

10. Dassot, M., Fournier, M., Deleuze, C.: Assessing the scaling of the tree branch diameters frequency distribution with terrestrial laser scanning: methodological framework and issues. Annals of Forest Science **76**, 1–10 (2019)

11. Delagrange, S., Jauvin, C., Rochon, P.: Pypetree: A tool for reconstructing tree perennial tissues from point clouds. Sensors **14**(3), 4271–4289 (2014)

12. Du, S., Lindenbergh, R., Ledoux, H., Stoter, J., Nan, L.: Adtree: accurate, detailed, and automatic modelling of laser-scanned trees. Remote Sensing **11**(18), 2074 (2019)

13. Fan, G., Nan, L., Chen, F., Dong, Y., Wang, Z., Li, H., Chen, D.: A new quantitative approach to tree attributes estimation based on lidar point clouds. Remote Sensing **12**(11), 1779 (2020)

14. Fan, G., Nan, L., Dong, Y., Su, X., Chen, F.: Adqsm: A new method for estimating above-ground biomass from tls point clouds. Remote Sensing **12**(18), 3089 (2020)

15. Gorte, B.: Skeletonization of laser-scanned trees in the 3d raster domain. In: Innovations in 3D Geo Information Systems, pp. 371–380. Springer (2006)

16. Gorte, B., Pfeifer, N.: Structuring laser-scanned trees using 3d mathematical morphology. International Archives of Photogrammetry and Remote Sensing **35**(B5), 929–933 (2004)

17. Graham, B., Van der Maaten, L.: Submanifold sparse convolutional networks. arXiv preprint arXiv:1706.01307 (2017)

18. Guo, Y., Wang, H., Hu, Q., Liu, H., Liu, L., Bennamoun, M.: Deep learning for 3d point clouds: A survey. IEEE transactions on pattern analysis and machine intelligence **43**(12), 4338–4364 (2020)

19. Hackenberg, J., Spiecker, H., Calders, K., Disney, M., Raumonen, P.: Simpletree—an efficient open source tool to build tree models from tls clouds. Forests **6**(11), 4245–4294 (2015)

20. Huang, H., Wu, S., Cohen-Or, D., Gong, M., Zhang, H., Li, G., Chen, B.: L1-medial skeleton of point cloud. ACM Trans. Graph. **32**(4), 65–1 (2013)

21. Interactive Data Visualization, I.: The standard for vegetation modeling and middleware, `https://store.speedtree.com/`

22. Kankare, V., Holopainen, M., Vastaranta, M., Puttonen, E., Yu, X., Hyyppä, J., Vaaja, M., Hyyppä, H., Alho, P.: Individual tree biomass estimation using terrestrial laser scanning. ISPRS Journal of Photogrammetry and Remote Sensing **75**, 64–75 (2013)

23. Liu, Y., Guo, J., Benes, B., Deussen, O., Zhang, X., Huang, H.: Treepartnet: neural decomposition of point clouds for 3d tree reconstruction. ACM Transactions on Graphics **40**(6) (2021)

24. Livny, Y., Yan, F., Olson, M., Chen, B., Zhang, H., El-Sana, J.: Automatic reconstruction of tree skeletal structures from point clouds. In: ACM SIGGRAPH Asia 2010 papers, pp. 1–8. ACM (2010)

25. Molina-Valero, J.A., Martínez-Calvo, A., Villamayor, M.J.G., Pérez, M.A.N., Álvarez-González, J.G., Montes, F., Pérez-Cruzado, C.: Operationalizing the use of tls in forest inventories: The r package fortls. Environmental Modelling & Software **150**, 105337 (2022)

26. Paszke, A., Gross, S., Massa, F., Lerer, A., Bradbury, J., Chanan, G., Killeen, T., Lin, Z., Gimelshein, N., Antiga, L., et al.: Pytorch: An imperative style, high-performance deep learning library. Advances in neural information processing systems **32** (2019)

27. Qi, C.R., Yi, L., Su, H., Guibas, L.J.: Pointnet++: Deep hierarchical feature learning on point sets in a metric space. Advances in neural information processing systems **30** (2017)

28. Raumonen, P., Kaasalainen, M., Åkerblom, M., Kaasalainen, S., Kaartinen, H., Vastaranta, M., Holopainen, M., Disney, M., Lewis, P.: Fast automatic precision tree models from terrestrial laser scanner data. Remote Sensing **5**(2), 491–520 (2013)

29. Ronneberger, O., Fischer, P., Brox, T.: U-net: Convolutional networks for biomedical image segmentation. In: International Conference on Medical image computing and computer-assisted intervention. pp. 234–241. Springer (2015)

30. Saha, P.K., Borgefors, G., di Baja, G.S.: A survey on skeletonization algorithms and their applications. Pattern recognition letters **76**, 3–12 (2016)

31. Spalding, E.P., Miller, N.D.: Image analysis is driving a renaissance in growth measurement. Current opinion in plant biology **16**(1), 100–104 (2013)

32. Tang, H., Liu, Z., Li, X., Lin, Y., Han, S.: Torchsparse: Efficient point cloud inference engine. Proceedings of Machine Learning and Systems **4**, 302–315 (2022)

33. Tompalski, P., Coops, N.C., White, J.C., Goodbody, T.R., Hennigar, C.R., Wulder, M.A., Socha, J., Woods, M.E.: Estimating changes in forest attributes and enhancing growth projections: a review of existing approaches and future directions using airborne 3d point cloud data. Current Forestry Reports **7**, 1–24 (2021)

34. Verroust, A., Lazarus, F.: Extracting skeletal curves from 3d scattered data. In: Proceedings Shape Modeling International'99. International Conference on Shape Modeling and Applications. pp. 194–201. IEEE (1999)

35. White, J.C., Wulder, M.A., Vastaranta, M., Coops, N.C., Pitt, D., Woods, M.: The utility of image-based point clouds for forest inventory: A comparison with airborne laser scanning. Forests **4**(3), 518–536 (2013)

36. Xu, H., Wang, C.C., Shen, X., Zlatanova, S.: 3d tree reconstruction in support of urban microclimate simulation: A comprehensive literature review. Buildings **11**(9), 417 (2021)

37. Xu, H., Gossett, N., Chen, B.: Knowledge and heuristic-based modeling of laser-scanned trees. ACM Transactions on Graphics (TOG) **26**(4), 19–es (2007)

38. Zahid, A., Mahmud, M.S., He, L., Heinemann, P., Choi, D., Schupp, J.: Technological advancements towards developing a robotic pruner for apple trees: A review. Computers and Electronics in Agriculture **189**, 106383 (2021)